

Supporting Information

Anisotropic Circular Dichroism of Jet-Cooled Chiral Molecules

Changseop Jeong, Jiyeon Yun, Jiyoung Heo,* and Nam Joon Kim*

Two factors that may affect the circular dichroism (CD) values in the resonant two-photon ionization (R2PI) CD measurements

Two factors that may affect the R2PICD values measured using our molecular beam apparatus are described herein. These factors are (1) asymmetry within the detection efficiencies of the time-of-flight (TOF) mass spectrometer for the ions generated by left- and right-handed circularly polarized (LCP and RCP, respectively) pulses, and (2) linear dichroism due to the linear polarization (LP) components in the LCP and RCP beams.

(1) Detection asymmetry of the TOF mass spectrometer

The asymmetry in the detection efficiencies of the TOF mass spectrometer was recognized by observing the variation in the CD values at different voltage settings of the X-deflector in the TOF mass spectrometer (Fig. S1).

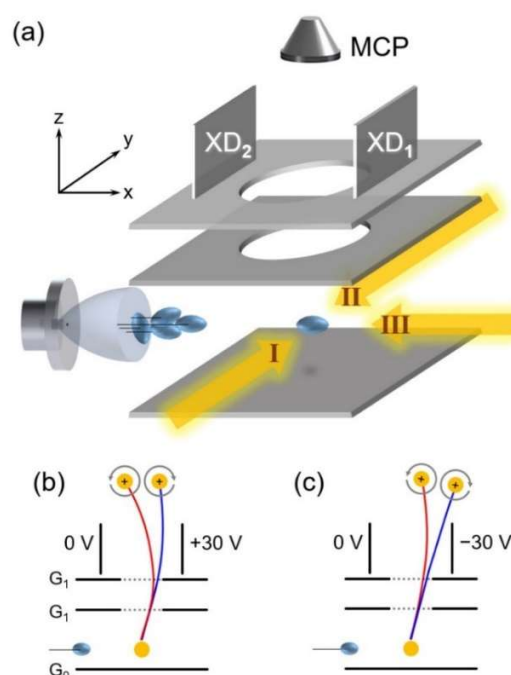


Figure S1. (a) Schematic diagram of the TOF mass spectrometer. I, II, and III represent three different directions of the propagation of the UV beam. X-deflector comprises two electrodes: XD₁ and XD₂. The ion trajectories generated by LCP (red line) and RCP (blue line) pulses in the direction I were illustrated when the XD₁ voltage was set to (b) +30 V and (c) -30 V, and the XD₂ was grounded. It was assumed that the molecules were ionized via transition to the P branch.

The X-deflector comprises two electrodes: XD₁ and XD₂. XD₂ was grounded and XD₁ was set to a voltage that gives the highest ion signals by steering the ion trajectories to a microchannel plate (MCP) with an active area diameter of 18 mm.

Figure S2a shows the R2PI (upper) and R2PICD (lower) spectra of AG(a), AG(b), and GG(a) of (1*S*,2*S*)-(+)–pseudoephedrine ((+)PED) obtained using the dual-beam method with CP and LP beams propagating in the direction I (Fig. S1).

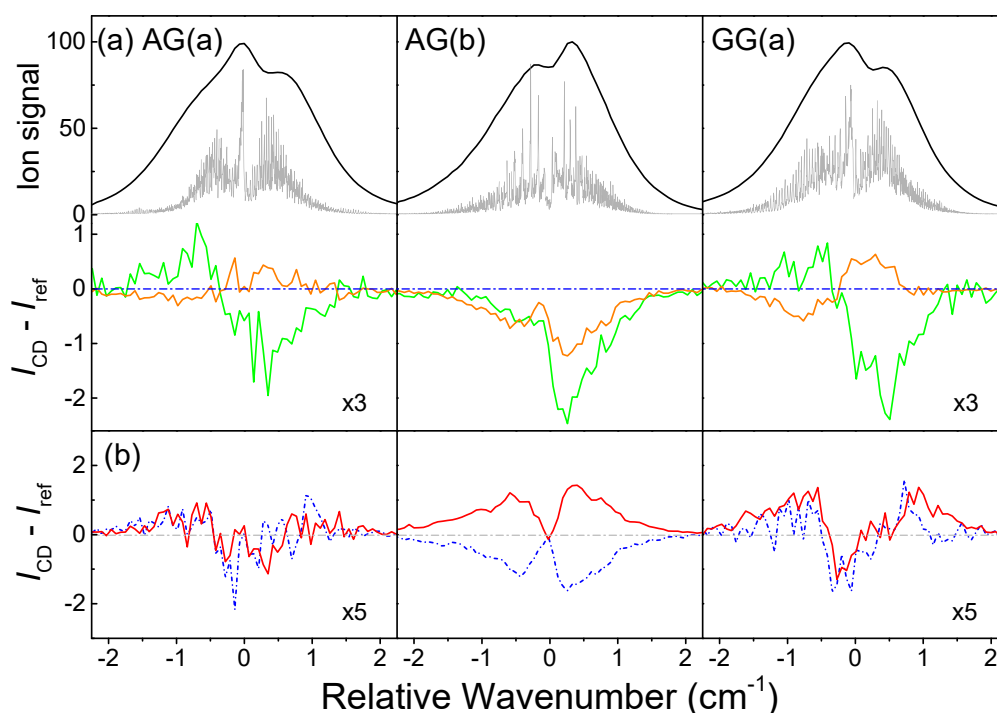


Figure S2. (a) R2PI (upper) and R2PICD (lower) spectra of AG(a), AG(b), and GG(a) of (+)PED. The simulated rotational band contours are overlapped with the origin bands. The R2PICD spectra were obtained with two different voltage settings of the X-deflector. With XD₂ grounded, the XD₁ voltage was set to -30V (green) and +30V (orange). (b) R2PICD spectra of AG(a), AG(b), and GG(a) of (+)PED (blue dot) and (1*R*,2*R*)-(–)–PED ((–)PED) (red line) obtained using the CP beam counterpropagating to the molecular beam pulse (III in Fig. S1).

The spectra were obtained by scanning the origin bands of the (+)PED conformers using a UV laser with a step size of 0.07 cm⁻¹. The CD values of the origin band of AG(b) are all negative, consistent with the previous report,¹ whereas the CD signs of AG(a) and GG(a) change within the single origin bands. Furthermore, the CD values varied with the variation of

the XD_1 voltage. For instance, the CD values of the P and R branch decrease and increase, respectively, with altering the XD_1 voltage from -30 V to $+30$ V. As a result, the CD signs of the P and R branches of AG(a) and GG(a) measured with the XD_1 voltage of -30 V become opposite to those with the voltage of $+30$ V.

These results indicate that the detection efficiencies of the ions generated by the LCP and RCP pulses in the TOF mass spectrometer are not identical. They vary depending on the voltage settings of the X-deflector. These different detection efficiencies of the ions generated by the LCP and RCP pulses may be caused by their different ion trajectories toward the MCP after the X-deflector, although the reason for this difference in the ion trajectories has not been clearly understood yet.

We speculate that this phenomenon may be connected to the orientation of the J vectors of ions produced when molecules absorb LCP and RCP pulses. In the case of a symmetric top molecule, which is preferentially excited by LCP and RCP pulses in either the P or R branch, the J vector is almost parallel to the propagation direction of the CP beam (Fig. 2).² This means the rotation axis of the molecule aligns almost parallel to the CP beam's propagation direction but perpendicular to the electric field direction in the X-deflector (Fig. S1).

Moreover, the J vector's orientation, excited by LCP and RCP pulses, is opposite to each other. Therefore, if the ions generated by RCP pulses rotate clockwise, those generated by LCP pulses will rotate counterclockwise (Figs. S1b–c). We assume that the fragment ions rotate in the same direction as the parent ions, considering that the R2PICD spectra of PED were obtained by monitoring the fragment ions at m/z 58.

The molecules generated by supersonic expansion have velocities of a few hundred meters per second along the x-axis. Consequently, the ions produced by R2PI will also have the same velocity along the x-axis. These ions are then accelerated perpendicularly along the z-axis by the electric field in the ionization region, moving toward the field-free region of the TOF

mass spectrometer. Upon passing through the X-deflector, the ions are deflected either toward XD₁ or XD₂, depending on the polarity of the XD₁ voltage (Fig. S1).

The rotational motion of ions around an axis perpendicular to the electric field vector of the X-deflector can influence the deflection angles of the ions passing through it. When ions are generated by LCP and RCP pulses, they rotate counterclockwise and clockwise, respectively. As a result, they are deflected at different angles by the electric field of the X-deflector, leading to different ion trajectories in the field-free region. This variation in trajectories causes the ions to arrive at different positions in the active area of the MCP (Fig. S1). Some ions may not even reach the active area of the MCP, which leads to an increase in the asymmetry in the detection efficiency.

When molecules are excited to the R branch, the directions of the *J* vectors of the ions generated by LCP or RCP pulses become opposite to those of the molecules excited to the P branch.^{2,3} These contrasting *J* vectors in the P and R branches might result in opposite trends in CD variations as the XD₁ voltage is changed from -30 V to +30 V (Fig. S2a).

This speculation about the phenomenon is supported by the observation that when the direction of the CP beam's propagation was changed to II (Fig. S1a), the CD signs and the variation trend in the P and R branches with the XD₁ voltage were reversed. This means that the CD values of the P and R branch increased and decreased, respectively, with altering the XD₁ voltage from -30 V to +30 V. Furthermore, when the direction of the CP beam's propagation was changed to III, i.e., counterpropagating to the molecular beam pulse (III in Fig. S1), the variations in the CD values at different voltage settings of the X-deflector disappeared. This disappearance of the CD variations may occur because the *J* vectors of the molecules excited to the P and R branches become parallel to the propagation vector of the CP beam and, consequently, to the electric field vector of the X-deflector. Thus, the different directions of the rota-

tional motion, i.e., clockwise or counterclockwise, may have little effect on the deflection angles of the ions passing through the X-deflector.

Further investigation is necessary to confirm this hypothesis and clarify the reason for the asymmetry in the detection efficiency. All R2PICD spectra in Figure 1 were obtained with a CP beam counterpropagating to the direction of the molecular beam pulses (III in Fig. S1).

(2) Linear dichroism

Figure S2b shows the R2PICD spectra of the conformers of (+)PED and (–)PED irradiated by CP beams, which counterpropagate to the direction of the molecular beam pulse. Although the CD values of the P and R branches did not vary with the XD₁ voltage, the CD spectra of AG(a) and GG(a) showed that (+)PED and (–)PED are not mirror images. These nonmirror image CD spectra are due to the contribution of linear dichroism, which is comparable to or larger than the CD of the origin bands of AG(a) and GG(a). The CD spectra of AG(b) exhibit mirror images, which may result because the contribution of linear dichroism is smaller than the CD of AG(b).

We found that the linear dichroism arose due to the LP components in the LCP and RCP beams, which were generated when a CP beam passed through a fused silica window in the molecular beam chamber. Figure S3a shows the ellipticities of the LCP and RCP pulses generated using a photoelastic modulator (PEM), showing that the majority of the light is CP light with few LP components. However, when we placed a fused silica window (thickness=10 mm) after the PEM, numerous LP components were generated in the LCP and RCP pulses (Fig. S3b). These results indicate that LP components could be generated when the CP pulses pass through a fused silica window (thickness=10 mm) installed in the molecular beam apparatus. The relative amounts of LP components decreased with decreasing thickness of the window. For instance, when the 10-mm-thick window was replaced with a 1-mm-thick one, the relative

amounts of the LP components to the CP components greatly reduced. The mirror image R2PICD spectra between (+)PED and (-)PED in Figure 1 were obtained using 1-mm-thick fused silica windows installed in the molecular beam apparatus.

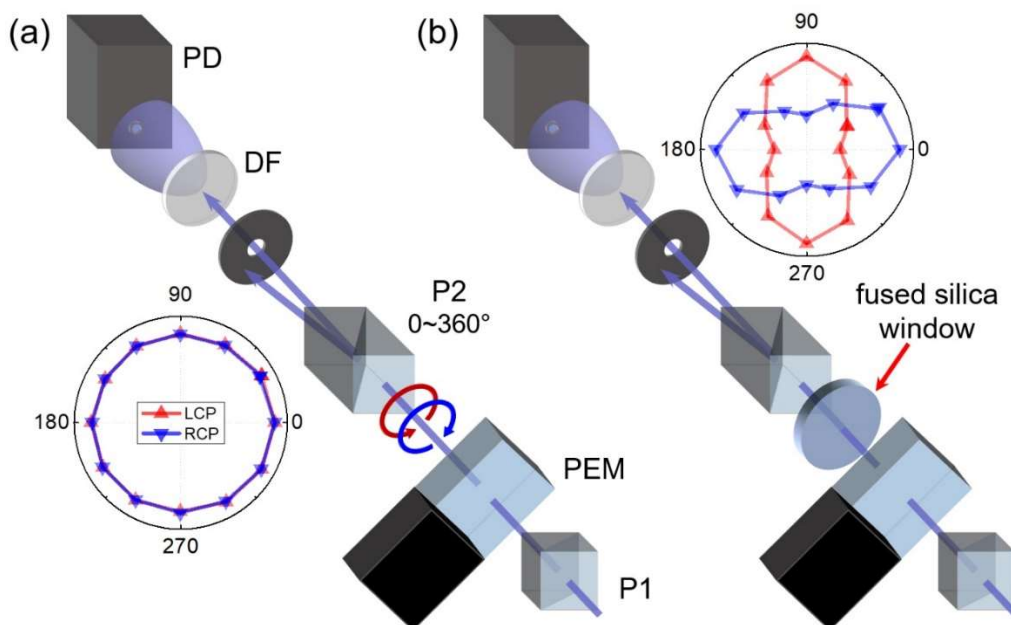


Figure S3. Schematic diagrams of the ellipticity measurement setups (a) without and (b) with a fused silica window (thickness=10 mm) after the PEM, which was placed between two Rochon polarizers P1 and P2. The ellipticities of LCP and RCP pulses were measured by monitoring the intensity of the ordinary beam after P2 as a function of the polarization angle of P2 with respect to that of P1. A fused silica diffuser (DF, Edmund optics) was used to avoid an error from the spatial gain variation of a photodiode (PD). The inset shows the ellipticities of LCP and RCP pulses. The ellipticities of LCP and RCP pulses generated using the PEM without the fused silica window display nearly CP light with little LP component. In contrast, a large amount of LP component was generated in LCP and RCP pulses when the fused silica window was placed after the PEM.

References

1. A. Hong, C. M. Choi, H. J. Eun, C. Jeong, J. Heo and N. J. Kim, *Angew. Chem. Int. Ed.*, 2014, **53**, 7805-7808.
2. C. Jeong, K. K. Mishra, J. Yun, J. Heo and N. J. Kim, *Bull. Korean Chem. Soc.*, 2022, **43**, 369-375.
3. K. L. Han, *Phys. Rev. A*, 1997, **56**, 4992-4995.